

Table S1. List of antibodies used for characterization of mucosal mononuclear and epithelial cells in rhesus macaques.

Antibody	Isotype	Clone	Working Dilution	Source	Method Used
Anti-human CD3 Pacific Blue	Mouse IgG1	SP34-2	1:2	BD Biosciences	FC
Anti-human CD3	Rabbit polyclonal	-	1:100	Biocare Medical	IF
Anti-human CD4 APCH7	Mouse IgG1	L200	1:1	BD Biosciences	FC
Anti-human CD11c	Mouse IgG1	3.9	1:50	Biologend	IF
Anti-human CD45	Mouse IgG1	D058-1283	1:50	BD Biosciences	IF
Anti-human CD45 APC	Mouse IgG1	MB4-6D6	1:11	Miltenyi Biotec	FC
Anti-human CD68	Mouse IgG1	KP1	1:50	Dako	IF
Anti-human CD79a	Mouse IgG1	HM47	1:100	BD Biosciences	IF
Anti-human CD210 (IL10R)	Rat IgG2a	3F9	1:100	Biologend	IF
Anti-human CD210 (IL10R) PE	Rat IgG2a	3F9	1:1	Biologend	FC
Anti-human IL10	Rat IgG1	JES3-9D7	1:20	Biologend	IF
Anti-human IL10 PE-Cy7	Rat IgG1	JES3-9D7	1:1	Biologend	FC
Anti-human IFN γ	Mouse IgG1	4S.B3	1:20	Biologend	IF
Anti-human IFN γ PerCP-Cy5.5	Mouse IgG1	4S.B3	1: 10	BD Biosciences	FC
Anti-phospho-STAT3	Rabbit IgG	D3A7	1:50	Cell Signaling	IF
Anti-human TNF α	Mouse IgG1	MAB11	1:20	Biologend	IF
Anti-human TNF α Alexa Flour 700	Mouse IgG1	Mab11	1:2	BD Biosciences	FC
Active Caspase 3	Rabbit polyclonal	-	1:500	Abcam	IF
Anti-human ZO-1	Mouse IgG1	ZO1-1A12	1:30	Invitrogen	IF
Anti-cow Cytokeratin, Wide Spectrum Screening	Rabbit polyclonal IgG	-	1:500	Dako	IF

IOPath [®] Cytokeratin- Large Spectrum	Mouse IgG1	KL1	1:50	Beckman Coulter	IF
Anti-Human Epithelial Antigen FITC	Mouse IgG1	Ber-EP4	1:2	Dako	FC

Note: Before all staining, the dilution of the respective antibodies was determined via serial dilution experiments. IF and FC represent immunofluorescence and flow cytometry respectively.

Table S2: Percentages of active caspase-3 positive enterocytes detected in normal and acute SIV infected rhesus macaques.

Category	Animal Number	Tissue	Days post SIV infection	AC-3+ enterocytes (%) (mean \pm standard errors)	
Normal	GB61	Colon	-	1.0 \pm 0.3	
	GJ06	Colon	-	0.5 \pm 0.1	
	GN70	Colon	-	1.1 \pm 0.2	
	GN74	Colon	-	0.9 \pm 0.1	
	FF15	Colon	-	0.6 \pm 0.1	
	FF23	Colon	-	0.3 \pm 0.1	
	GB61	Jejunum	-	2.3 \pm 0.7	
	GJ06	Jejunum	-	0.2 \pm 0.1	
	GN70	Jejunum	-	3.2 \pm 1.1	
	GN74	Jejunum	-	1.8 \pm 0.8	
	FF15	Jejunum	-	0.2 \pm 0.1	
	FF23	Jejunum	-	0.4 \pm 0.1	
	Acute SIV Infection	AV63	Colon	8	0.8 \pm 0.2
		AV85	Colon	21	4.1 \pm 0.7
AV91		Colon	10	0.7 \pm 0.3	
BA17		Colon	13	2.3 \pm 0.5	
BA57		Colon	8	1.3 \pm 0.2	
BN37		Colon	21	0.5 \pm 0.1	
HN29		Colon	10	1.7 \pm 0.2	
M992		Colon	13	2.0 \pm 0.4	
AV63		Jejunum	8	10.9 \pm 1.5	
AV85		Jejunum	21	18.0 \pm 3.0	
AV91		Jejunum	10	10.5 \pm 1.9	
BA17		Jejunum	13	8.6 \pm 3.2	
BA57		Jejunum	8	11.5 \pm 4.3	
BN37		Jejunum	21	14.3 \pm 3.8	
HN29	Jejunum	10	6.8 \pm 1.2		
M992	Jejunum	13	11.0 \pm 3.5		

SUPPLEMENTARY FIGURES:

Figure S1: Interferon gamma ($\text{IFN}\gamma$) expression of CD3^+ T-cells and CD3^- lymphocytes in jejunum lamina propria mononuclear cells detected by flow cytometry from a representative macaque at day 0 and 21 days post $\text{SIV}_{\text{MAC251}}$ infection. (A) Cells were gated first on singlets, lymphocytes, followed by live cells and then on CD3^+ T-cells and CD3^- lymphocytes. (B) The percentages of total $\text{IFN}\gamma$ are shown in each upper box of each plot of CD3^+ T-cells and CD3^- lymphocytes. (C) The percentages for $\text{IFN}\gamma$ are shown for CD3^+ T-cells and CD3^- lymphocytes (open histograms) along with fluorescence minus controls (filled histograms).

Figure S2. Linear regression analysis was performed comparing mean percentages of active caspase-3+ enterocytes and plasma viral load in acute (A & C) and chronic (B & D) SIV infected macaques. Note there is an inverse correlation between apoptotic enterocytes and plasma viral load during acute phase of infection in both colon (A, n=8) and jejunum (C, n=8). Interestingly, a positive correlation is shown between apoptotic enterocytes and plasma viral load during chronic infection in both colon (B) and jejunum (D) tissues (n=7). However, these data were not statistically significant.

Figure S3. Jejunum villus height, crypt length, and villus to crypt ratio, and colon crypt length and breadth in both normal, and SIV-infected macaques. Differences in jejunum villus height (A), jejunum crypt length (B), jejunum villus:crypt ratios (C), colon crypt length (D), and colon crypts breadth (E) with means \pm standard errors were plotted from normal, and SIV-infected animals. Increased jejunum and decreased colon crypt length were detected in acute (n=6) and chronic (n=6) SIV infected macaques compared

to uninfected controls (n=7). A minimum of 12 to 20 fields from each animal was considered for morphometric analysis. Asterisks indicate statistically significant differences between the respective animal groups (* denotes $p < 0.005$ and ** denotes $p < 0.0001$).

Figure S4. Detection of p-STAT3 positive cells in normal and SIV infected jejunum tissues. Phosphorylated-STAT3 positive cells were detected in uninfected normal (A), acute (B) and chronic (C) SIV-infected macaques by immunohistochemistry staining using anti-pSTAT3 monoclonal antibodies with nuclear fast red counterstain. (D) Isotype control developed with Mach 3 Rabbit AP-Polymer staining showed no positive brown staining in tissues. Black arrow denotes the presence of pSTAT3 positive cells (dark brown color), majority distributed in lamina propria region.

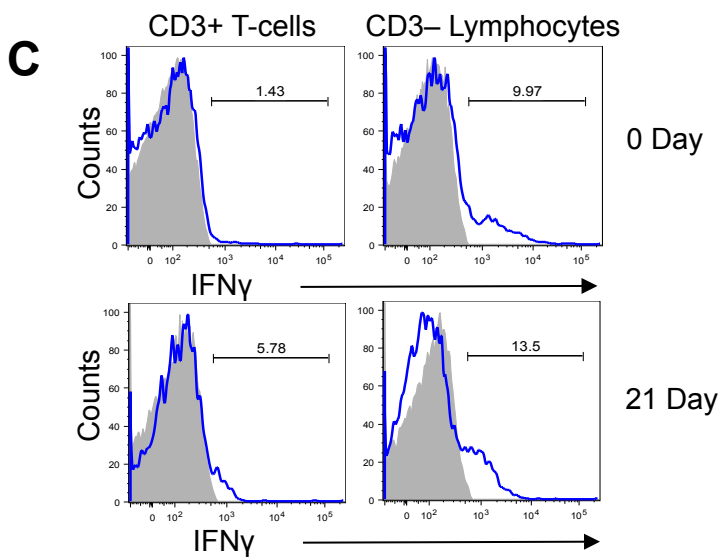
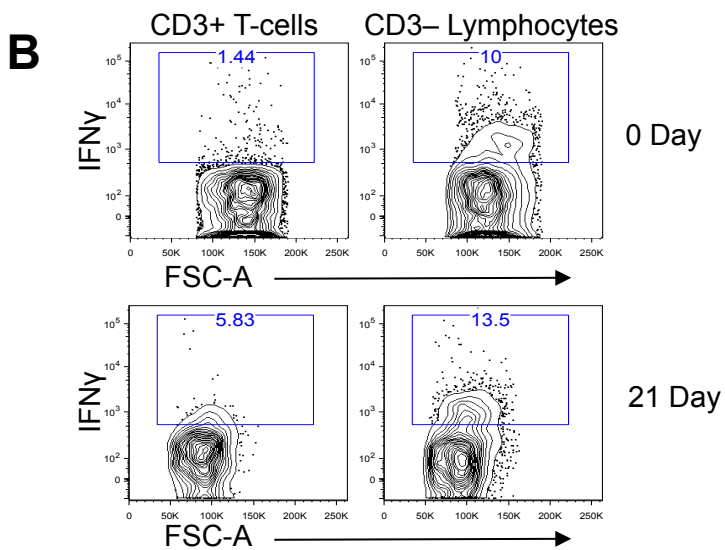
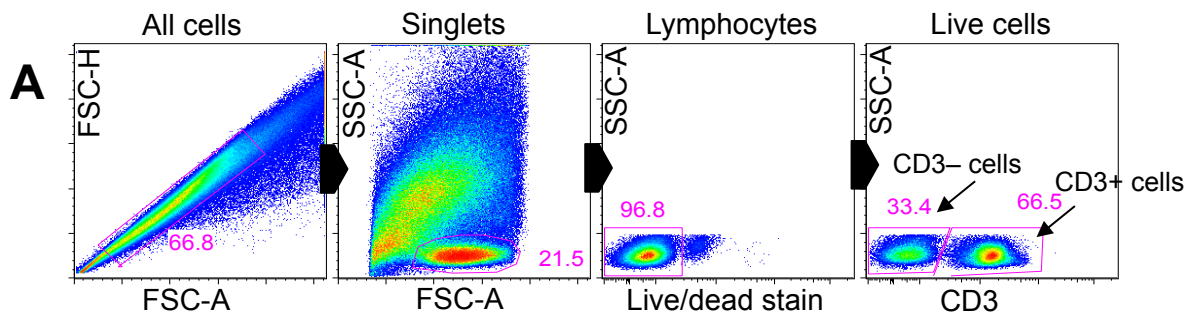


Figure S1

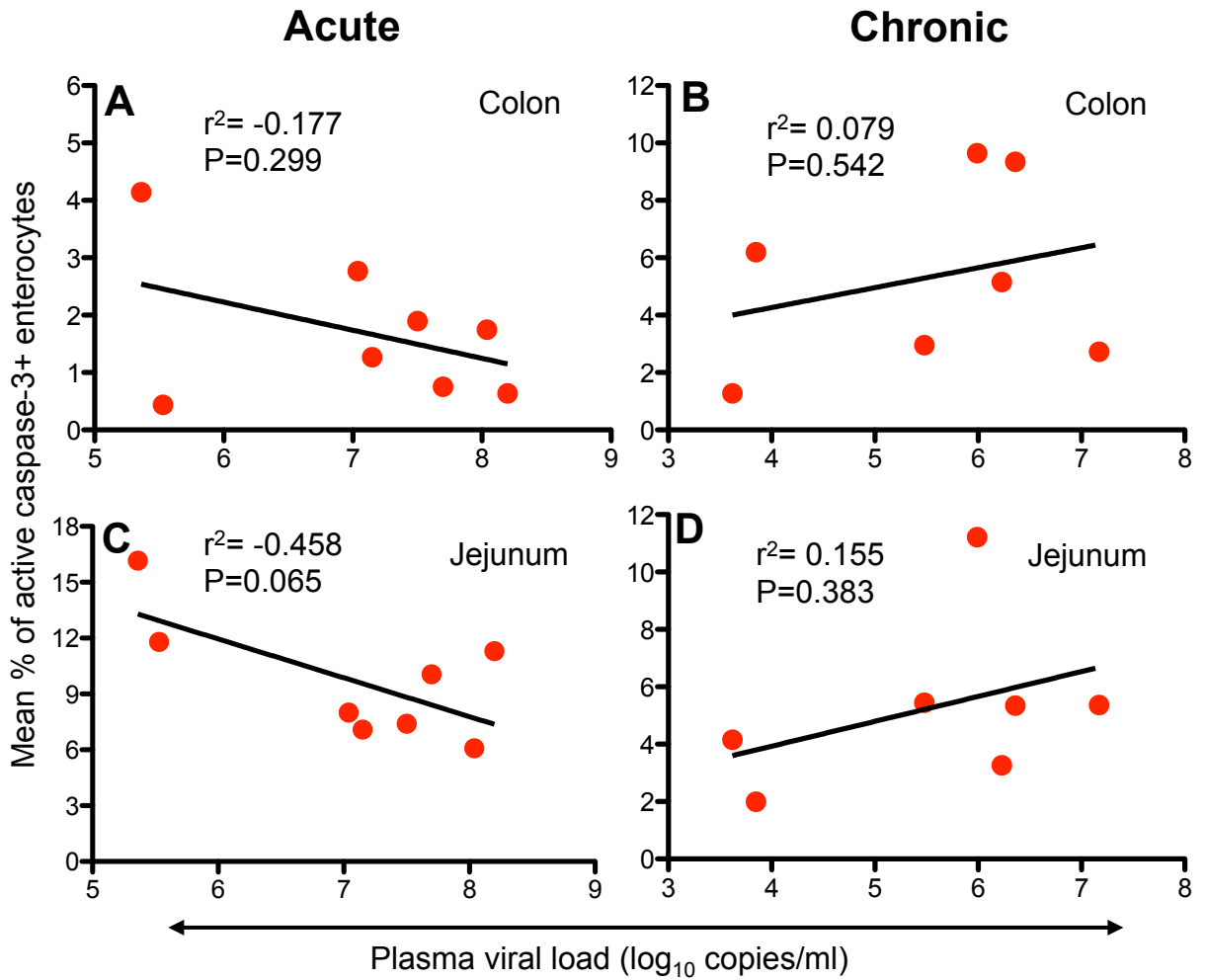


Figure S2

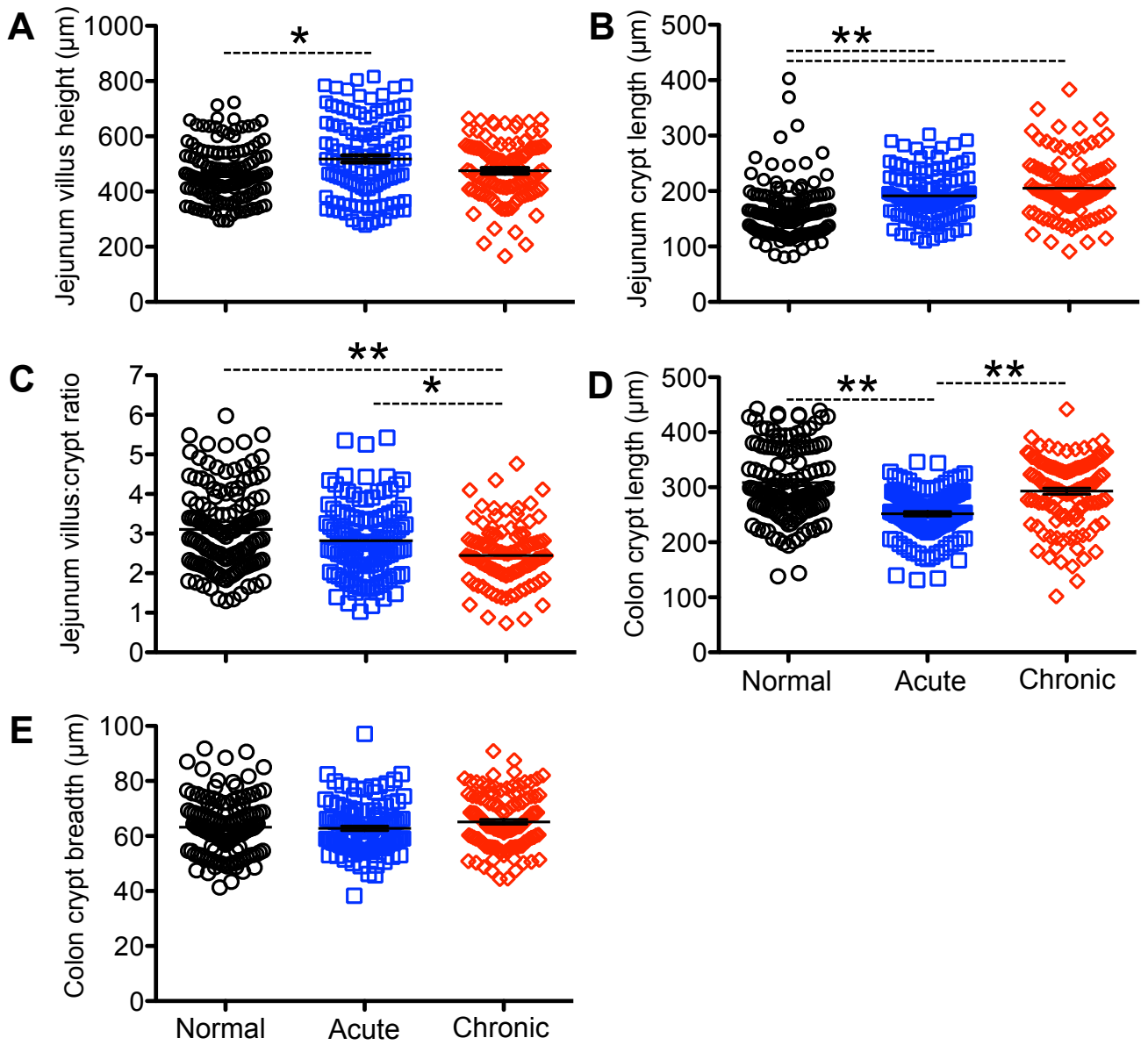


Figure S3

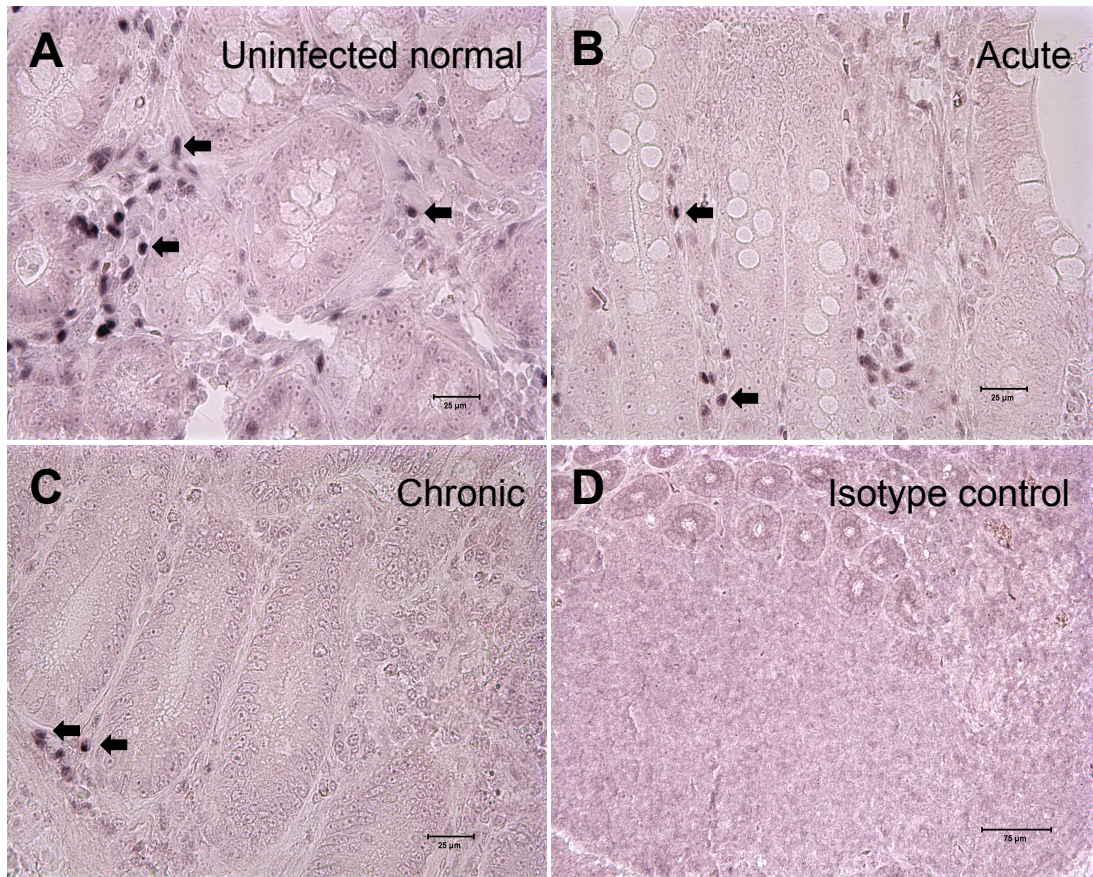


Figure S4